Photoluminescence under pressure of ultrathin AlAs layers grown on GaAs vicinal surfaces: A search for lateral confinement effects

B. Chastaingt, M. Leroux, G. Neu, N. Grandjean, C. Deparis, and J. Massies
Laboratoire de Physique du Solide et Energie Solaire, CNRS, F06560 Valbonne, France
(Received 7 August 1992)

In $Al_{0.3}Ga_{0.7}As$/GaAs quantum wells bordered by ultrathin (one or two monolayers) AlAs layers, the AlAs layer has been shown to provide a well for electrons at high pressure [Phys. Rev. B **45**, 11 846 (1992)]. In this work, the same type of structures, but grown on (001) substrates misoriented towards (111)Ga, are studied by photoluminescence as a function of pressure, and a comparison is made with those grown on nominal substrates in order to investigate the influence of surface steps on electronic levels. Particular emphasis is given to indirect type-II transitions. An important blueshift of indirect transitions is observed in the case of two AlAs monolayers grown on a vicinal substrate. The size of this shift may be explained considering diffusion of carriers by the interface steps, or also lateral confinement. Inversely, a redshift is observed in the one AlAs monolayer sample. We suggest that this last point may be due to terrace length fluctuations.

I. INTRODUCTION

Semiconductor heterostructures exhibiting two-dimensional confinement (i.e., quantum wires) have been the object of extensive research, both experimentally[1–5] and theoretically,[6–9] not only in the framework of novel physical properties, but also in view of their technological applications. Increased carrier mobilities[6] and low lasing threshold[9] [relative to quantum wells (QW's)] are expected from these structures; lasers incorporating quantum wires have already been demonstrated.[5] On the other hand, some intrinsic limitations have been put forward that could prevent the expected improvement of optoelectronic properties.[10] Various methods may be used in order to obtain these geometries, such as *e*-beam lithography or reactive ion etching[3,10] (with or without overgrowth), patterned Ga implantation,[11] and epitaxial growth on patterned substrates.[5] In particular, epitaxial growth on misoriented substrates has been used for the elaboration of quantum-wire arrays,[1] corrugated interface QW's,[2] tilted superlattices,[12] and serpentine superlattices.[13]

In a recent high-pressure photoluminescence (PL) study,[14] it was shown that in single $Al_{0.3}Ga_{0.7}As/AlAs/GaAs/AlAs/Al_{0.3}Ga_{0.7}As$ double-barrier quantum wells (DBQW's), ultrathin [one or two monolayers (ML)] AlAs layers can form a well and bind electrons. This is due to the large valence-band offset between GaAs and AlAs on one side, and $Al_{0.3}Ga_{0.7}As$ and AlAs on the other side, in addition to the large X_z electron mass. Under pressure, this results in a type-II configuration, where electrons and holes are not confined in the same layer of the heterostructure. It was observed that the monolayers or bilayers of AlAs on nominal surfaces could be considered as uniform within the experimental limits. Moreover, it was shown that the electron confinement energy in one and two AlAs monolayers was satisfactorily obtained via the envelope-function formalism. If such structures are grown on a vicinal (001) surface with a regular array of steps, it appears that the height of the atomic steps (1 ML) is of the same order of magnitude as the width of the confining potential for electrons (1–2 ML), as sketched in Fig. 1. This can prove useful for studying lateral confinement effects in the high confinement limit. In particular, it should be noted that such additional lateral confinement affects

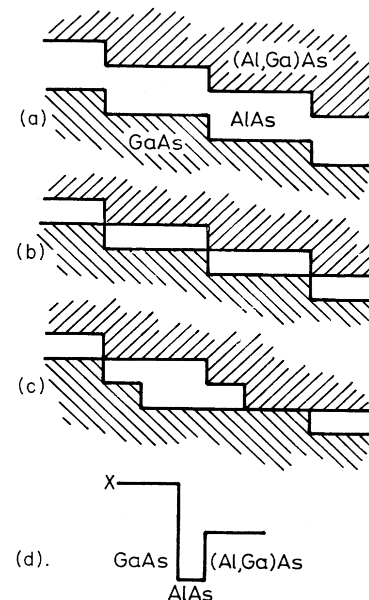

FIG. 1. Schematics of ultrathin AlAs layers sandwiched between GaAs and $Al_{0.3}Ga_{0.7}As$ on vicinal surfaces. (a) Two AlAs ML on an ideal vicinal surface. (b) One AlAs ML on an ideal vicinal surface. (c) A simplified view of the effect of step growth of one AlAs ML on a vicinal surface exhibiting terrace length disorder. (d) The scheme of the X conduction band of $GaAs/AlAs/Al_{0.3}Ga_{0.7}As$ heterostructures (strain effects are omitted for simplicity).

 ©1993 The American Physical Society

only electrons, whereas holes stay confined in a broader GaAs quantum well.

This work reports a high-pressure PL study of the same DBQW structures as those studied in Ref. 14, but grown on (001) substrates slightly misoriented toward (111)Ga. The results are compared with those obtained on structures grown in the same run on nominal (001) substrates. Particular emphasis is given to the type-II pressure regime, in order to study the influence of steps on the electron states confined in ultrathin AlAs QW's.

After a brief presentation of the experimental part of this work (Sec. II), the results will be presented in Sec. III and discussed in Sec. IV.

II. EXPERIMENT

Details of the molecular-beam epitaxy (MBE) of the samples can be found in Refs. 14 and 15. The samples consisted of a 1-μm-thick GaAs buffer layer followed by three GaAs QW's of width 80, 40, and 20 Å embedded in 500-Å-thick $Al_{0.3}Ga_{0.7}As$ barriers. At each well-barrier interface, a thin AlAs layer of width one monolayer [samples DBQW (1 ML)] or two monolayers [samples DBQW (2 ML)] is inserted. The high-pressure PL properties of the samples grown on nominal substrates are discussed in Ref. 14. Two pieces of the same misoriented substrate were used for the two misoriented samples studied. Nominal and vicinal substrates were placed at the same distance from the center of the rotating substrate holder, in order to improve homogeneity among samples. The vicinal substrate misorientation is 4° toward (111)Ga (40-Å average step distance). This misorientation (where edges are oriented along the [−110] axis) is known to favor smooth step edges[16–18] and results in optimized optical properties relative to the perpendicular misorientation toward (111)As.[18–20]

PL was measured at 5 K in a diamond anvil cell using argon as a pressure transmitting medium. It was excited using the 4880-Å line of an argon laser and detected using a cooled GaAs photocathode photomultiplier. Details of the experimental setup can be found in Refs. 14 and 21.

III. RESULTS

Before presenting the high-pressure PL properties of the QW's grown on vicinal surfaces, we recall their PL properties at ambient pressure. Whereas the PL spectra of QW's grown on substrates misoriented toward (111)As exhibit strong redshift and a substantial broadening, this is not the case for QW's grown on (111)Ga substrates.[18,19,22] Indeed, sharp features are obtained for this latter kind of misorientation, due to "pseudosmooth" interfaces.[19] However, again for the latter case, whereas the QW luminescence lies at about the same (or slightly redshifted) energy as that of QW's grown on nominal substrates, a systematic blueshift of PL excitation line energies is observed. This blueshift is slightly sample dependent, but the overall trend is a decrease with well-width increase.[18,23] This is shown in Fig. 2 for various QW samples on 4° misoriented samples. This blueshift of intrinsic transitions has recently been interpreted as being due to the scattering of carriers due to the superlattice

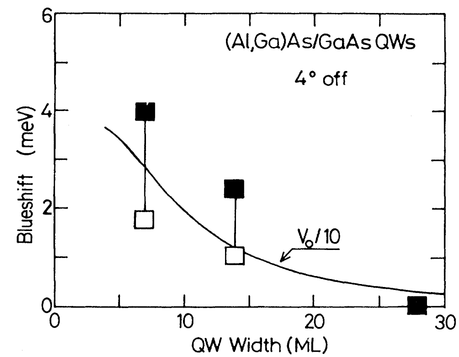

FIG. 2. Blueshift of the e_1hh_1 PL excitation lines for various $Al_{0.3}Ga_{0.7}As/GaAs$ quantum wells grown on a 4° off-substrate relative to wells grown on nominal substrates. Experimental data are from Refs. 18 (closed symbols) and 23 (open symbols). The solid line results from the model in Appendix A.

potential induced by the interface steps.[23] In Appendix A, we propose a simple approach to this problem that will prove useful in the rest of this paper. The result of this model, shown as a solid line in Fig. 2, gives a reasonable account of the atmospheric pressure experimental observations on $Al_{0.3}Ga_{0.70}As/GaAs$ QW's.

We now turn to the high-pressure PL properties of DBQW's grown on vicinal surfaces. We shall start with the comparison of samples DBQW (2 ML) (i.e., with two AlAs monolayers on both sides of the well) grown on nominal and vicinal surfaces (hereafter nominal and vicinal samples). The PL spectra of samples DBQW (2 ML) at two different pressures are compared in Figs. 3(a) and 3(b). At 1.3 GPa [Fig. 3(a)], the 80- and 40-Å-wide wells are direct (type I) and are slightly redshifted in the vicinal

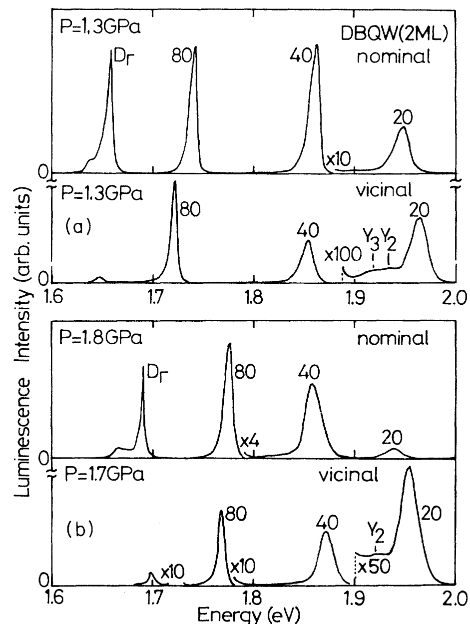

FIG. 3. Photoluminescence spectra at 1.3 and 1.8 GPa of QW's bordered by two AlAs monolayers [DBQW (2 ML)] grown on nominal and vicinal substrates.

sample relative to the nominal one. In contrast, the 20-Å-wide well is indirect (type II, with the electron in the AlAs bilayer[14]), and the PL of the well in the vicinal sample is now blueshifted (by 20 meV) relative to the nominal one. At 1.8 GPa [Fig. 3(b)], both the 40- and 20-Å-wide wells are indirect, and a similar blueshift of the wells of the vicinal sample is observed. Another point to be noted in Fig. 3 is that the intensity of type-II wells relative to that of type I at a given pressure is lower in the vicinal sample than in the nominal one. Also, phonon coupling appears to be stronger. In Fig. 3, the phonon replica labeled $Y2$ and $Y3$, following the notation of Skolnick *et al.*,[24] correspond to GaAs-like and AlAs-like optical phonons.

The pressure dependence of the PL transition energies of the vicinal sample DBQW (2 ML) are given in Fig. 4. In this figure, the transitions labeled D_Γ and NX correspond, respectively, to donor-bound and nitrogen-bound exciton recombinations in bulk GaAs.[14,25,26] These transitions can serve as an internal pressure calibration, though pressure is monitored by the $R1$ ruby luminescence scale.[27] Linear least-squares fits of the QW transition energies are shown as solid lines in Fig. 4. Also shown as dashed lines are the results obtained for the nominal sample, as given in Ref. 14. The PL energies of the direct (type-I) wells are nearly the same in the nominal and vicinal samples. Actually, due to the large pressure coefficient of Γ transitions (≈ 100 meV/GPa), the slight differences observed are within the precision of the ruby scale. On the other hand, Fig. 4 shows evidence of a systematic and large blueshift of type-II PL transitions of the vicinal sample for the three GaAs well widths. The pressure dependence of type-II transition energies of both samples is given in Table I. On the average, the blueshift is 20 meV for the well width of 20 Å, and 19 meV for that of width 40 Å. Only a few data points are available for the 80-Å-wide well, but their blueshift is also 20 meV on average. As mentioned in Ref. 14, in each sample the electron state involved in the type-II PL recombination is of the same kind for the three wells, i.e., a confined state in a 2-ML AlAs well [see Fig. 1(d)]. It is then reasonable to conclude that the large blueshift measured is mainly due to an increase in the electron confinement energy.

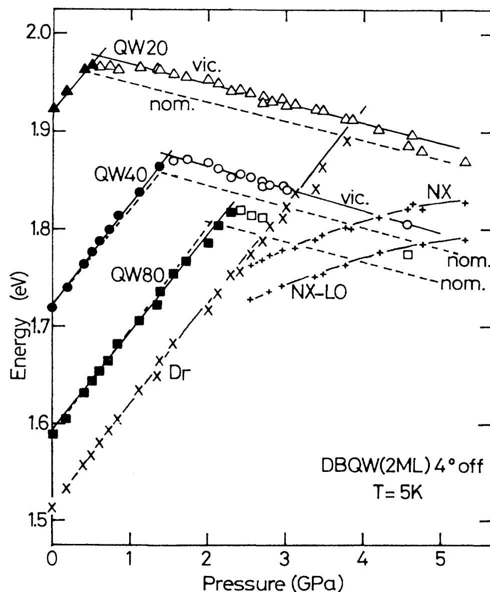

FIG. 4. Pressure dependence of the luminescence energies of QW's bordered by two AlAs monolayers grown on a vicinal surface. The solid lines are least-squares fits to the data. For comparison, the same data for a sample grown on a nominal substrate (Ref. 14) are shown as dashed lines.

We now turn to the sample DBQW (1 ML), i.e., with one AlAs ML border. It should be noted that in the nominal sample, the electron confinement energy in AlAs is large [189 meV (Ref. 14)], resulting in a very low binding energy relative to the $Al_{0.3}Ga_{0.7}As$ barrier (increasing with pressure between 5 and 10 meV). Qualitatively, any increase in confinement energy due to the step array, as reported above, will push the electron state nearer to the barrier level, resulting in a spreading of the wave function in the barrier, and eventually a delocalization. A decrease in the type-II optical oscillator strength is then expected.

Figure 5 compares the PL spectra of nominal and vicinal DBQW (1 ML) samples at $P \approx 1.5$ GPa. At that pressure, the 20-Å-wide well is type II. A strong decrease of type-II PL intensity of the vicinal sample is observed. However, contrary to the preceding case, the type-II PL of the vicinal sample [Fig. 5(b)] is *redshifted* relative to the nominal one [Fig. 5(a)]. Moreover, in Figs. 5(b) and 5(c) we show the spectra of two different pieces of the vicinal sample (two different pressure runs). The type-II transitions in both chips exhibit a stronger phonon coupling than the nominal sample, but the line shapes are different. In Fig. 5(b), the zero phonon line is stronger, but in Fig. 5(c), phonon replicas are more intense than the zero phonon line [in the language of short-period superlattices, the spectrum of Fig. 5(b) is that of a pseudodirect transition, and that of Fig. 5(c) of an indirect transition[28]]. This can be considered as an illustration of disorder and inhomogeneities in this sample, as discussed below (Sec. IV).

Spectra at a higher pressure (3.4 GPa) are shown in Fig. 6. At this pressure, all three wells in samples

TABLE I. Pressure dependence of type-II transition energies in the nominal (Ref. 14) and vicinal samples [$E(P)=E(0)+\alpha_X P$].

Sample	GaAs well width (Å)	$E(0)$ (eV)	α_X (meV/GPa)
DBQW (2 ML) vicinal	20	1.990	−20
	40	1.910	−23
DBQW (2 ML) nominal	20	1.969	−19.7
	40	1.888	−21.3
DBQW (1 ML) vicinal	20	1.987	−18
DBQW (1 ML) nominal	20	2.002	−19.2

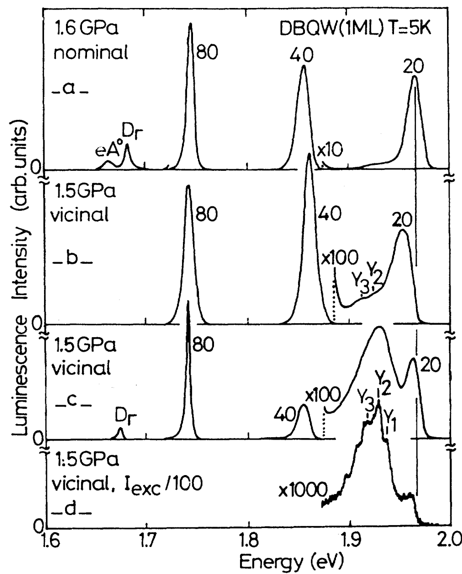

FIG. 5. Photoluminescence spectra at $P \approx 1.5$ GPa of QW's bordered by one AlAs monolayer [DBQW (1 ML)] grown on nominal and vicinal substrates.

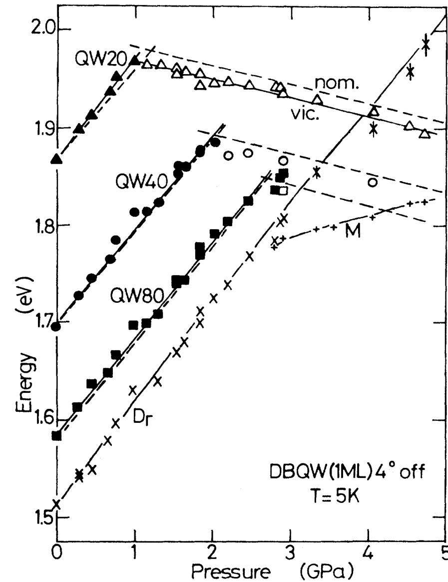

FIG. 7. Pressure dependence of the photoluminescence energies of QW's bordered by one AlAs monolayer grown on a vicinal substrate. Solid lines are fits to the data. For comparison, the results of a sample grown on a nominal sample (Ref. 14) are shown as dashed lines.

DBQW (1 ML) are type II. It should be noted that, whereas in the nominal sample emission from the three QW's is still detectable and as intense as PL from the buffer,[14] in the vicinal sample the QW PL is almost totally quenched, except for a weak signal from the 20-Å well that is again redshifted relative to the nominal sample well. Actually, the PL of the vicinal sample at high pressure is dominated by transitions originating from the GaAs bulk, which is principally composed of a multiplet labeled *M* in Figs. 6 and 7. This multiplet, of unknown origin, does not seem to include single nitrogen-bound excitons (*NX*, detected in the other samples), since we do not observe the typical phonon train of *NX* (with a Huang-Rhys factor of 0.3). However, nitrogen is likely to take part in this feature, exhibiting the same pressure dependence as *NX* (compare Figs. 7 and 4). The *M* photoluminescence feature appears as an efficient recombination channel in bulk GaAs, and the energy of the GaAs direct excitonic gap was measured by absorption, as shown in Fig. 6. However, apart from the differences in buffer PL, the point we want to emphasize in Fig. 6 is that, regarding QW PL intensities at high pressure, the vicinal DBQW (1 ML) sample is more similar to that of QW's grown without AlAs (shown in Fig. 6 for comparison) than to that of the nominal sample, i.e., QW luminescence is almost totally quenched.

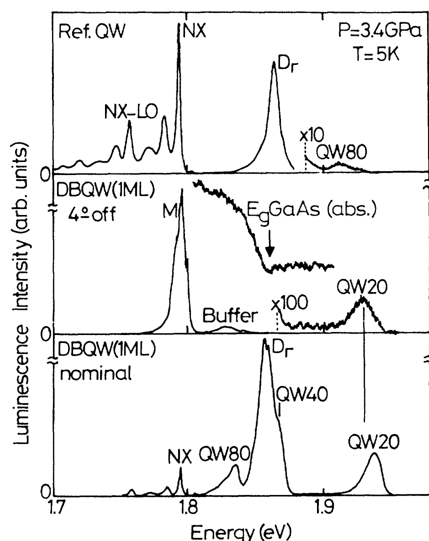

FIG. 6. Comparison of the photoluminescence spectra at 3.4 GPa of QW's bordered by one AlAs monolayer grown on nominal and vicinal substrates. Also shown is the spectrum of a standard $Al_{0.3}Ga_{0.7}As/GaAs$ QW (i.e., with no AlAs borders).

The pressure dependence of the PL energies of sample DBQW (1 ML) are plotted in Fig. 7. As in Fig. 4, solid lines denote fits to the data on the vicinal sample, whereas dashed lines are fits obtained to the nominal one (from Ref. 14). Indirect transitions originating from the 40- and the 80-Å well are also redshifted in the vicinal sample relative to the nominal one. However, due to overlap with the broad phonon train of the 20-Å well, it is not clear whether the type-II transitions of the 40- and 80-Å wells reported in Fig. 7 are zero phonon lines. The energy pressure relation of the 20-Å well in both samples is given in Table I.

IV. DISCUSSION

From the preceding section, it is clear that due to the different results obtained in the two series of samples, they should be discussed separately.

Since one of the main effects expected from the additional confinement provided by steps on electrons in AlAs wells is a blueshift, it is easier first to discuss samples DBQW (2 ML). The most important feature observed is a blueshift of 19–20 meV of type-II transitions for the sample grown on the vicinal surface. Since the confinement energy of electrons on nominal 1- and 2-ML-wide wells is experimentally known (189 and 144 meV, respectively[14]), the model of Appendix A can be used. Using Eq. (A2), a blueshift of the electron state of 4 meV is expected. Adding the hole contribution results in expected blueshifts of 6 and 5 meV for the 20- and 40- (and 80) -Å-wide wells. It is rather fair that a simple perturbative treatment without adjustable parameters gives the right order of magnitude in a situation corresponding to the complicated geometry shown in Fig. 1(a). However, the effect of steps is underestimated. A possible reason for this can be found by inspecting Fig. 1. For very small well widths (we are dealing with 1- or 2-ML electron wells), the definition of the perturbing potential in Appendix A may no longer be valid. Actually, for a 1-ML-wide well, this potential is the difference between the bottom of the AlAs conduction band and that of the barrier ($\approx$210 meV) as shown in Fig. 1(b) [using this limiting potential height and Eq. (A2) gives blueshifts of 18 and 17 meV for the 20- and 40- (and 80) -Å wells; however, the rather good agreement with experiment is fortuitous, since a perturbative approach is not valid in this case].

So far, steps have been considered as generating an array of diffusive potentials for carriers. The other extreme situation is when carriers are confined by the steps, i.e., the quantum-wire case. In Appendix B we show the simplest model of an isolated two AlAs ML wide quantum wire.[8] Though, as stated in the Appendix, the approximations made are very rough, and the model potential used hardly reflects the actual situation, we shall use it to get an idea of the lateral dimension involved in lateral confinement, if there is any. A blueshift of 20 meV would correspond to a quantum wire $\approx$ 55-Å wide according to Fig. 9. This rough agreement with the step length (40 Å) shows that the lateral confinement can also provide an explanation of the large high-energy shift of type-II transitions measured in the vicinal DBQW (2 ML) sample.

On the other hand, it can be seen in Fig. 9 that lateral confinement pushes the ground state X_z level of the AlAs well toward higher-lying X_{xy} states (either confined states or the barrier level). This increases the mixing between these states. It is known from uniaxial stress experiments that X_x and X_{xy} states do mix in short-period nominal superlattices.[29] The intentional presence of surface steps in our sample is expected to increase this mixing. This can tentatively explain the stronger phonon coupling of type-II transitions in the vicinal sample reported in Fig. 3.

We shall now discuss the results obtained with samples DBQW (1 ML). In Sec. III, we have shown that type-II photoluminescence is almost totally quenched in the vicinal sample, but is shifted toward lower energies relative to the nominal sample. As already stated, since the binding energy of electrons relative to the $Al_{0.3}Ga_{0.7}As$ barrier is very low (5–10 meV), no blueshift as high as for sample DBQW (2 ML) can be expected (using the model in Appendix A leads to increased energies of only 0.5–1 meV for electrons). However, any pushing of electron levels nearer to the $Al_{0.3}Ga_{0.7}As$ level will result in a greater spreading of the electron wave function in the barrier, and then a decrease in the type-II radiative lifetime.[14] This may provide a first explanation of the low PL efficiency of the vicinal sample (and also, as previously, to the stronger phonon coupling). But repulsive superlattices or lateral confinement effects, even weak, cannot explain a redshift. A first explanation for this could be poor quality of the vicinal DBQW (1 ML) sample, resulting in a strong localization of excitons. This cannot be discarded, since even the GaAs buffer PL spectra are different between the nominal and vicinal samples, as shown in Fig. 6.

Another tentative explanation can be given that relies on specific growth mechanisms of molecular-beam epitaxy (step flow growth). On a nominal sample, 1-ML islands are formed that accommodate incident atoms at their edges (steps) until coalescence. On a vicinal substrate, misorientation-induced steps provide the nucleation sites for step flow. The result of the step flow growth of one AlAs ML on a misoriented surface exhibiting terrace length disorder is schematized in Fig. 1(c). The terrace length fluctuates around its average value imposed by the misorientation angle. This is the simplest type of disorder to be envisaged, and it is experimentally known to exist even in surfaces misoriented toward (111)Ga.[17] From Fig. 1(c), it can be seen that idealized step flow growth of one AlAs ML on such a surface results in strong chemical disorder: regions appear with no AlAs at all, whereas wires 2 ML wide are also formed. Obviously, various situations can be encountered and the transition energies associated with them have been calculated using the envelope-function formalism and the same approximations as in Ref. 14, that have proven successful in accounting for the nominal sample case. From these calculations, it appears that the pressure dependence of the PL energy of the type-II 20-Å-wide well in the vicinal sample DBQW (1 ML) is well accounted for either by considering sample regions with no AlAs (barrier conduction band to heavy hole in the GaAs well with no AlAs border), or also by considering transitions involving an electron in a two AlAs ML wide quantum wire. In the latter case, the wire is estimated to be $\approx$50 Å large, using the approximations of Appendix B. These two situations are shown in Fig. 1(c). In fact, step-induced disorder, at the scale of a 1-ML-wide QW, can lead to many different configurations, all of which we have not considered. But the point we wanted to stress is that the simple example of disorder sketched in Fig. 1(c) may give an explanation to the observation of PL transitions lower in energy in the vicinal than in the nominal DBQW (1 ML) sample.

At this point, three explanations for the poor type-II PL efficiency of the vicinal DBQW (1 ML) sample may be given: (i) the pushing of the electron states toward the barrier level, resulting in an increase in radiative lifetime (this tends to the case of a type-II QW with no AlAs monolayer[14]); (ii) the low filling factor of disordered islands seen in luminescence; and (iii) the lower sample

quality, resulting in shorter nonradiative lifetimes, cannot be discarded.

V. CONCLUSIONS

The influence of monomolecular potential steps on the electronic properties of the ultrathin electron quantum wells has been studied through the high-pressure type-II photoluminescence in double-barrier $Al_{0.3}Ga_{0.7}As$/AlAs/GaAs quantum wells grown on substrates misoriented by 4° toward (111)Ga. A strong increase in electron confinement energy of ≈ 20 meV due to the barrier steps has been observed in two AlAs monolayer wide wells. Simple envelope-function arguments, involving either carrier diffusion by step, or even step-induced lateral confinement, can account for the size of this effect. On the other hand, in the case of one AlAs monolayer wide electron wells grown on a vicinal surface, a strong quenching of type-II PL intensity is observed that may be due to the pushing of electron states toward the barrier level. The lower energies of type-II transitions observed in this case may be satisfactorily accounted for by considering the chemical disorder, induced by step disorder, at the monolayer scale. It is expected that other growth conditions, for instance use of optimum misorientation angles,[18] can improve this latter result.

Finally, it should be noted that sample geometries can be constructed where the type-II configuration (with electrons in the ultrathin AlAs layer) is the ground state at atmospheric pressure. The findings about such samples will be the object of a future paper.

ACKNOWLEDGMENT

This work was supported in part by the commission of European Communities (Contract No. ST2J-3F).

APPENDIX A

In this appendix, a simple approach to the problem of blueshifted transitions in QW's grown on vicinal surfaces (relative to nominal surfaces), without adjustable parameters, will be given. It is very tractable and gives a reasonable account of the experimental observations for QW's larger than the terrace width (Fig. 2). The main ideas are the same as those of Ref. 23; that is, a perturbative model in which the step arrays are represented by a repulsive potential superlattice.

As shown in Fig. 8, an ideal representation of the growth of a perfect n-ML-wide QW grown on a regular array of steps results in a regular squeezing of the QW width (this is an explanation for the repulsive nature of the potential). As also sketched in Fig. 8, since this squeezing occurs only on one regularly spaced lattice site, it may be represented as the usual Dirac comb. Still from a perturbative point of view, the potential strength V_0 can be approximated by the difference in confinement energies between an $(n-1)$ and an n monolayer wide well:

$$V_0 \approx V_{0e} + V_{0h} = E_e(n-1) - E_e(n) + E_{hh}(n-1) - E_{hh}(n) , \quad (A1)$$

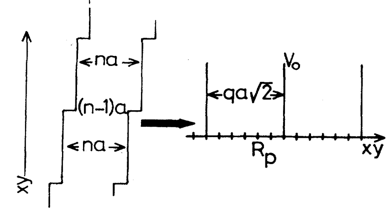

FIG. 8. Scheme of a wide QW grown on a regular array of steps, and of the model potential used.

where $E_e(n)$ $[E_{hh}(n)]$ are the confinement energies of electrons (holes) in an n-ML-wide QW. In this expression, the influence of steps on both electrons and holes has been included (we neglect the influence of steps on the exciton Rydberg). Since this definition gives a potential with the dimension of an energy, it has to be expended on a lattice (see Fig. 8): $V(R_p) = \Sigma_r V_0 \delta_{p,rq}$ with p, q, and r integers and δ the dimensionless Kronecker symbol.

Using $R_p = x$ and $R_{rq} = rqa/\sqrt{2}$ (where a is the step height, i.e., half the zinc-blende lattice constant, and the $\sqrt{2}$ term comes from the fact that the step edges are along $[-110]$) and with the usual summation rules,[30] one obtains

$$V(x) = V_0 a\sqrt{2} \Sigma_r \delta(x - rqa\sqrt{2}) ,$$

where $\delta(x)$ is the Dirac distribution. This leads to the standard formulation of the Kronig-Penney Hamiltonian:

$$H = p^2/2m - \Sigma_r (\hbar^2 \alpha / md) \delta(x - rd) ,$$

with m the in-plane effective mass and $d = qa\sqrt{2}$ the superlattice period. The secular equation is

$$\cos(Kd) = \cos(k) - \alpha(k^{-1}) \sin(k) , \quad (A2)$$

where k is related to the energy via $E = \hbar^2 k^2 / 2md^2$. For small α and small k, the ground-state energy ($K=0$) is simply given by

$$E = V_0/q = V_0 tg(\theta)\sqrt{2} , \quad (A3)$$

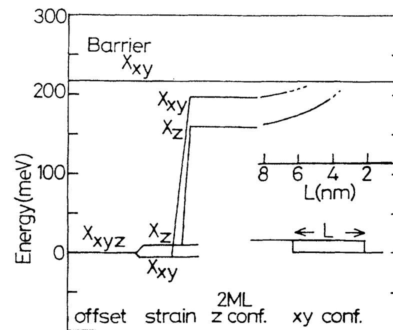

FIG. 9. Energy levels of a two AlAs ML thin quantum wire as a function of wire width. Strain, z confinement, and xy confinement effects as a function of wire width L are shown.

where θ is the misorientation angle. This approximation is valid for the QW's shown in Fig. 2. For $\theta=4°$, the curve corresponding to $E=V_0/10$ [with V_0 calculated using the envelope-function formalism and Eq. (A1)] gives the right order of magnitude for the blueshift of excitonic transitions, at atmospheric pressure, of large QW's grown on vicinal surfaces (Fig. 2).

APPENDIX B

In this appendix, the simplest case of a quantum wire will be considered.[8] It supposes that the xy,z dependence of the potential is simply the sum of z-dependent potential and an xy-dependent one. Obviously, this overestimates the potential strength involved in our case (see Fig. 1), since it totally neglects interwire coupling. Actually, instead of a potential well in the corners of the ultrathin structure, this model supposes high barriers. We shall simply use this model in order to see if lateral confinement (quantum-wire) effects are consistent with the lateral dimension of the step array (40 Å).

Using the envelope-function formalism, and the above approximation (where z- and xy-confinement energies are simply added[8]) gives the diagram of Fig. 9. Relative to the lower $Al_{0.30}Ga_{0.7}As$ barrier level, we show the effect on the AlAs X conduction-band state of the band offset, the epitaxial biaxial strain, the confinement in the growth axis (z) direction, and the lateral (xy) confinement. Since the above model can lead to energies higher than the barrier level, only results for wide wires are shown in Fig. 9.

[1] M. Tsuchiya, J. M. Gaines, R. H. Yan, R. J. Simes, P. O. Holtz, L. A. Coldren, and P. M. Petroff, Phys. Rev. Lett. **62**, 466 (1989).
[2] M. Tanaka and H. Sakaki, Jpn. J. Appl. Phys. **27**, L2025 (1988).
[3] A. Izrael, B. Sermage, J. Y. Marzin, A. Ougazzaden, R. Azoulay, J. Etrillard, V. Thierry-Mieg, and L. Henry, Appl. Phys. Lett. **56**, 830 (1990).
[4] A. Forchel, A. Mensching, B. E. Maile, H. Leier, and R. German, J. Vac. Sci. Technol. B **9**, 444 (1991).
[5] E. Kapon, D. M. Hwang, and R. Bhat, Phys. Rev. Lett. **63**, 430 (1989).
[6] H. Sakaki, Jpn. J. Appl. Phys. **19**, L735 (1980).
[7] J. A. Brum, G. Bastard, L. L. Chang, and L. Esaki, Superlatt. Microstruct. **3**, 47 (1987).
[8] U. Bockelmann and G. Bastard, Phys. Rev. B **45**, 1688 (1992).
[9] M. Asada, Y. Miyamoto, and Y. Suematsu, Jpn. J. Appl. Phys. **24**, L95 (1985).
[10] H. Benisty, C. M. Sotomayer-Torres, and C. Weisbuch, Phys. Rev. B **44**, 10 945 (1991).
[11] F. E. Prinz, G. Lehr, E. M. Frohlich, H. Schweizer, A. Forchel, and J. Straka, Superlatt. Microstruct. **11**, 321 (1992).
[12] T. Fukui and H. Saito, Jpn. J. Appl. Phys. **29**, L731 (1990).
[13] M. S. Miller, H. Weman, C. E. Pryor, M. Krishnamurthy, P. M. Petroff, H. Kroemer, and J. L. Merz, Phys. Rev. Lett. **68**, 3464 (1992).
[14] M. Leroux, N. Grandjean, B. Chastaingt, C. Deparis, G. Neu, and J. Massies, Phys. Rev. B **45**, 11 846 (1992).
[15] G. Neu, Y. Chen, C. Deparis, and J. Massies, Appl. Phys. Lett. **58**, 2111 (1991).
[16] P. Auvray, A. Poudoulec, M. Baudet, B. Guenais, A. Regreny, C. d'Anterroches, and J. Massies, Appl. Surf. Sci. **50**, 109 (1991).
[17] A. Poudoulec, B. Guenais, C. d'Anterroches, P. Auvray, M. Baudet, and A. Regreny, Appl. Phys. Lett. **60**, 2406 (1992).
[18] C. Deparis, Ph.D. thesis, Université de Grenoble, Grenoble, France, 1991 (unpublished).
[19] J. Massies, C. Deparis, C. Neri, G. Neu, Y. Chen, P. Auvray, and A. Regreny, Appl. Phys. Lett. **55**, 2605 (1989).
[20] Y. Chen, J. Massies, G. Neu, C. Deparis, and G. Neu, Solid State Commun. **81**, 877 (1992).
[21] M. Leroux, J. Leymarie, G. Neu, and G. Méheut, Rev. Sci. Instrum. **59**, 772 (1988).
[22] M. Colocci, M. Gurioli, A. Vinattieri, C. Deparis, J. Massies, and G. Neu, Appl. Phys. Lett. **57**, 783 (1990).
[23] F. Meseguer, N. Mestre, J. Sanchez-Dehesa, C. Deparis, G. Neu, and J. Massies, Phys. Rev. B **45**, 6942 (1992).
[24] M. S. Skolnick, G. W. Smith, I. L. Spain, C. R. Whitehouse, D. C. Herbert, D. M. Whittaker, and L. J. Reed, Phys. Rev. B **39**, 11 191 (1989).
[25] D. J. Wolford, in *Proceedings of the 18th International Conference on the Physics of Semiconductors, Stockholm, 1986,* edited by O. Engstrom (World Scientific, Singapore, 1986), p. 1115.
[26] J. Leymarie, M. Leroux, and G. Neu, Semicond. Sci. Technol. **4**, 235 (1989).
[27] A. Jayaraman, Rev. Sci. Instrum. **56**, 121 (1985).
[28] D. Scalbert, J. Cernogora, C. Benoit á la Guillaume, M. Maaref, F. F. Charfi, and R. Planel, Solid State Commun. **70**, 945 (1989).
[29] P. Lefebvre, B. Gil, H. Mathieu, and R. Planel, Phys. Rev. B **39**, 5550 (1989).
[30] J. Callaway, in *Quantum Theory of the Solid State* (Academic, New York, 1974), p. 352.